RESEARCH ARTICLE / НАУЧНАЯ СТАТЬЯ

Analytical model of deformation of reinforced concrete columns based on fracture mechanics

Ashot G. Tamrazyan[ID]✉, Vladimir I. Chernik[ID], Tatiana A. Matseevich[ID], Ivan K. Manaenkov[ID]

National Research Moscow State University of Civil Engineering, Moscow, Russian Federation

✉ tamrazian@mail.ru

Abstract. When conducting seismic calculations of reinforced concrete buildings and structures, it is quite important to use nonlinear models of structural performance, including those taking into account the overcritical operation in the fracture stage. The application of such models is especially important if the structures have an initial damage from fire or corrosion, as well as mechanical damage caused by force factors. The purpose of this study is to develop an analytical model of the deformation of eccentrically compressed reinforced concrete columns considering the stage of failure, which includes such processes as spelling of the protective layer, loss of stability of compressed reinforcement, and softening of confined concrete after reaching the design resistance. The existing models describing hysteresis behavior of reinforced concrete structures under low-cycle loading have been reviewed. The models have been analyzed in terms of considering the defining monotone curves, which are the boundaries of cyclic deformation. The model proposed in the research is constructed by analyzing the stages of the stress-strain state of a reinforced concrete column. At each stage, formulas are found for determining moment and curvature by solving equations of equilibrium of internal forces. Calculations based on the obtained model for a particular reinforced concrete column are carried out, monotonous diagrams are obtained, and a conclusion about the significant influence of the level of axial load on the character of deformation is made. On the basis of the obtained model, the construction of hysteresis diagrams under low-cycle loading is expected in the future.

Keywords: reinforced concrete column, deformation diagram, stages of destruction, hysteresis, seismic, low-cycle loads

Ashot G. Tamrazyan, Doctor of Technical Sciences, Professor, Head of the Department of Reinforced Concrete and Stone Structures, National Research Moscow State University of Civil Engineering, 26 Yaroslavskoye Shosse, Moscow, 129337, Russian Federation; ORCID: 0000-0003-0569-4788, Scopus Author ID: 55975413900, eLIBRARY SPIN-code: 2636-2447; tamrazian@mail.ru

Vladimir I. Chernik, postgraduate, lecturer, Department of Reinforced Concrete and Stone Structures, National Research Moscow State University of Civil Engineering, 26 Yaroslavskoye Shosse, Moscow, 129337, Russian Federation; ORCID: 0000-0001-6240-9993, Scopus Author ID: 57218420224, eLIBRARY SPIN-code: 5185-0373; chernik_vi@mail.ru

Tatiana A. Matseevich, Doctor of Physical and Mathematical Sciences, Associate Professor, Head of the Department of Applied Mathematics, National Research Moscow State University of Civil Engineering, 26 Yaroslavskoye Shosse, Moscow, 129337, Russian Federation; ORCID: 0000-0001-6292-0759, Scopus Author ID:51461741900, ResearcherID: AAB-2742-2020, eLIBRARY SPIN-code: 1299-6980; MatseevichTA@mgsu.ru

Ivan K. Manaenkov, Candidate of Technical Sciences, Associate Professor of the Department of Reinforced Concrete and Stone Structures, National Research Moscow State University of Civil Engineering, 26 Yaroslavskoye Shosse, Moscow, 129337, Russian Federation; ORCID: 0000-0002-5260-8793, Scopus Author ID: 57209888951, eLIBRARY SPIN-code: 5415-7373; ivanadekvatniy@mail.ru

Аналитическая модель деформирования железобетонных колонн на основе механики разрушения

А.Г. Тамразян, В.И. Черник, Т.А. Мацеевич, И.К. Манаенков

Национальный исследовательский Московский государственный строительный университет, Москва, Российская Федерация
✉ tamrazian@mail.ru

Аннотация. При проведении сейсмических расчетов железобетонных зданий и сооружений достаточно важным является применение нелинейных моделей работы конструкций, в том числе учитывающих закритическую работу в стадии разрушения. Особенно актуально применение таких моделей, если конструкции имеют начальные повреждения от пожара или коррозии, а также механические повреждения, вызванные силовыми факторами. Цель исследования – разработка аналитической модели деформирования внецентренно сжатых железобетонных колонн с учетом стадии разрушения, которая включает такие процессы, как откол защитного слоя, потеря устойчивости сжатой арматуры, разупрочнение ограниченного бетона после достижения расчетного сопротивления. Проведен обзор существующих моделей, описывающих гистерезисное поведение железобетонных конструкций при малоцикловом нагружении. Анализ моделей проводился в части рассмотрения определяющих монотонных кривых, которые являются границами циклического деформирования. Предлагаемая модель строится посредством анализа стадий напряженно-деформированного состояния железобетонной колонны. На каждой стадии находятся формулы для определения момента и кривизны путем решения уравнений равновесия внутренних сил. Проведен расчет на основе представленной модели для конкретной железобетонной колонны, получены монотонные диаграммы, сделан вывод о существенном влиянии уровня осевой нагрузки на характер деформирования. На основе полученной модели в дальнейшем предполагается построение диаграммы гистерезиса при малоцикловом нагружении.

Ключевые слова: железобетонная колонна, диаграмма деформирования, механика разрушения, гистерезис, сейсмика, малоцикловые нагрузки

Introduction

When performing calculations of reinforced concrete buildings and structures, it is quite important to apply non-linear methods of analysis which allow to ensure economical and reliable structures and to reveal reserves of bearing capacity of the system.

A widespread type of structural system used in seismic areas is the reinforced concrete frame, the feature of which is the perception of the horizontal component of seismic load due to the rigid joint between beams and columns.

In the nonlinear stage of frame frames, local areas of elastoplastic deformations occur in the vicinity of the girder support nodes. In accordance with this, in the design diagrams of frame frames, the nonlinear properties are concentrated in separate areas, which are called plastic joints, while the columns and spanning sections of the beams work elastically [1]. The appearance of plastic joints in columns in ordinary cases is considered to be unacceptable.

Тамразян Ашот Георгиевич, доктор технических наук, профессор, заведующий кафедрой железобетонных и каменных конструкций, Национальный исследовательский Московский государственный строительный университет, Российская Федерация, 129337, Москва, Ярославское шоссе, д. 26; ORCID: 0000-0003-0569-4788, Scopus Author ID: 55975413900, eLIBRARY SPIN-код: 2636-2447; tamrazian@mail.ru

Черник Владимир Игоревич, аспирант, преподаватель кафедры железобетонных и каменных конструкций, Национальный исследовательский Московский государственный строительный университет, Российская Федерация, 129337, Москва, Ярославское шоссе, д. 26; ORCID: 0000-0001-6240-9993, Scopus Author ID: 57218420224, eLIBRARY SPIN-код: 5185-0373; chernik_vi@mail.ru

Мацеевич Татьяна Анатольевна, доктор физико-математических наук, доцент, заведущая кафедрой прикладной математики, Национальный исследовательский Московский государственный строительный университет, Российская Федерация, 129337, Москва, Ярославское шоссе, д. 26; ORCID: 0000-0001-6292-0759, Scopus Author ID: 51461741900, ResearcherID: AAB-2742-2020, eLIBRARY SPIN-код: 1299-6980; MatseevichTA@mgsu.ru

Манаенков Иван Константинович, кандидат технических наук, доцент кафедры железобетонных и каменных конструкций, Национальный исследовательский Московский государственный строительный университет, Российская Федерация, 129337, Москва, Ярославское шоссе, д. 26; ORCID: 0000-0002-5260-8793, Scopus Author ID: 57209888951, eLIBRARY SPIN-код: 5415-7373; ivanadekvatniy@mail.ru

However, columns designed for elastic operation may suffer some damage during operation, e.g. caused by fire [2], reinforcement corrosion [3], mechanical damage, earthquake, etc. In such a case, due to the reduced mechanical characteristics, the behavior of the column in the elastic-plastic domain will have to be taken into account when carrying out verification calculations or justifying the reinforcement.

Description of nonlinear behavior of columns and beams in the plastic hinge region is usually carried out with the help of hysteresis diagrams (Figure 1), which take into account degradation of strength and stiffness at low-cycle vibrations, loss of dissipative energy, change of stiffness at opening and closing of cracks (pinching effect) [4]. Hysteresis diagrams are usually plotted in the axes "bending moment-curvature" or "horizontal force-horizontal displacement".

The basic element of a hysteresis diagram is the monotonic loading curve, commonly referred to as skeleton curves. The monotonic curve limits the range of possible deformation under low-cycle loading (Figure 1).

The monotonic curves should, wherever possible, take into account the greatest ductility of reinforced concrete structures and include areas of hardening and softening to establish the true nature of the redistribution of forces in the system.

Many hysteresis models of varying degrees of accuracy have been developed by individual researchers. Let's consider these models in terms of monotonic curves used.

In [5] a bilinear elastic-plastic diagram is proposed which has a linear-elastic first section with an equivalent stiffness Ke, after reaching the bearing capacity the stiffness becomes zero – a yield point occurs. The determination of the value of carrying capacity and equivalent stiffness for a particular structure is a rather complex task, for reinforced concrete columns the method proposed in [6] can be used. Despite its simplicity, the bilinear diagram [5] is quite popular for seismic calculations as it has clear computational advantages.
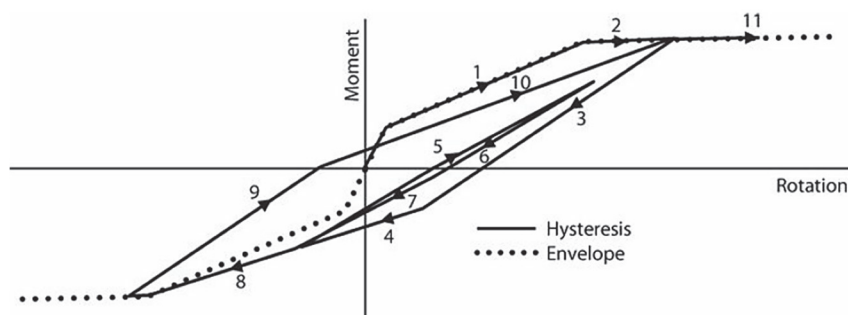

Figure 1. Hysteresis diagram based on the model of Takeda et al. [7]

In the bending of reinforced concrete columns and beams, the redistribution of stresses will cause the individual cross-sectional areas to engage gradually due to the non-linear behaviour of the reinforcement and the concrete. In this way, the bearing capacity of the elements will be realized and the possibility of absorbing a larger moment will be realized. In the deformation diagram, this can be accounted for by introducing a non-zero stiffness after the limit force is reached. This approach is implemented in the bilinear diagram proposed in [8]. The stiffnesses are usually determined by approximating real curvilinear diagrams obtained from experiments or numerical analysis. The bilinear diagram with strengthening combines computational simplicity and a more accurate account of strengthening effects, which justifies the choice of this model as the basis by other authors [9; 10].

A characteristic feature of reinforced concrete structures is the formation of normal and inclined cracks, which reduce the initial stiffness. In order to account for cracking, a three-line diagram of deformation has been proposed in [7] with a successive decrease in stiffness after the cracking force is reached and then when the yield strength in the reinforcement is reached. This approach makes it possible not only to take into account crack opening at the initial stages of deformation of the element, but also to provide a basis for describing the process of reopening and closing of cracks in subsequent cycles.

In addition to piecewise linear diagrams, some researchers use curvilinear diagrams in their models [11]. This allows a more accurate approximation of the real deformation diagram of the element and takes into account the consistent reduction of stiffness. In practice, this approach is less popular, which is justified by the complexity of the calculations and analysis of the results. It should also be noted that curvilinear diagrams have a rather narrow field of application, since the dependencies describing eccentrically compressed and bendable elements will be different.

Columns and beams adjacent to the frame nodes where the highest bending moments occur, according to the standards of most countries, must be reinforced by densely placed, closed cross clamps, which in addition to providing the strength of the sloping sections act as indirect reinforcement. The indirect reinforcement increases the load-bearing capacity of the elements and the plastic deformation capacity, which contributes to the redistribution of forces in the system and a fuller use of the load-bearing capacity reserves. In addition, after the limit forces are reached, when the stresses in the clamps reach the yield strength, there is no sudden failure of the element, but a gradual reduction in the bearing capacity with increasing plastic deformations follows [12]. Strengthening can take place when such phenomena as loss of stability of compressed reinforcement, geometric non-linearity, chipping of concrete cover layer are taken into account.

The described processes can be taken into account in models which include a branch of unstrengthening [13]. The model allows to take into account the true nature of force redistribution in the framework more accurately and is particularly relevant when carrying out the analysis of bearing capacity reserves for elements with initial damage [14].

The unstrengthening branch allows taking into account an important aspect of low-cycle operation of reinforced concrete elements, such as within-cycle degradation of strength. This is especially important in loading programs with sharply varying amplitudes, which can lead to sudden collapse of the structure.

The hysteresis diagrams were further developed in [15], which takes into account the presence of residual strength after unstrengthening, which is observed in tests of reinforced concrete structures under low-cycle loading. The presence of residual strength makes it possible to take into account the incomplete disconnection of an element from operation and an increase in the resilience of the structural system as a whole when performing calculations based on the criterion of no collapse.

It should be noted that the description of the reference points of hysteresis diagrams can be made in different ways. The most common approach is the approximation of experimental diagrams or by using empirical dependencies, e.g. in [15]. This method can also be applied in combination with diagrams derived from numerical calculations [14]. This somewhat limits the scope of application of the model and does not allow direct consideration of processes related to concrete rebound, loss of reinforcement stability, etc.
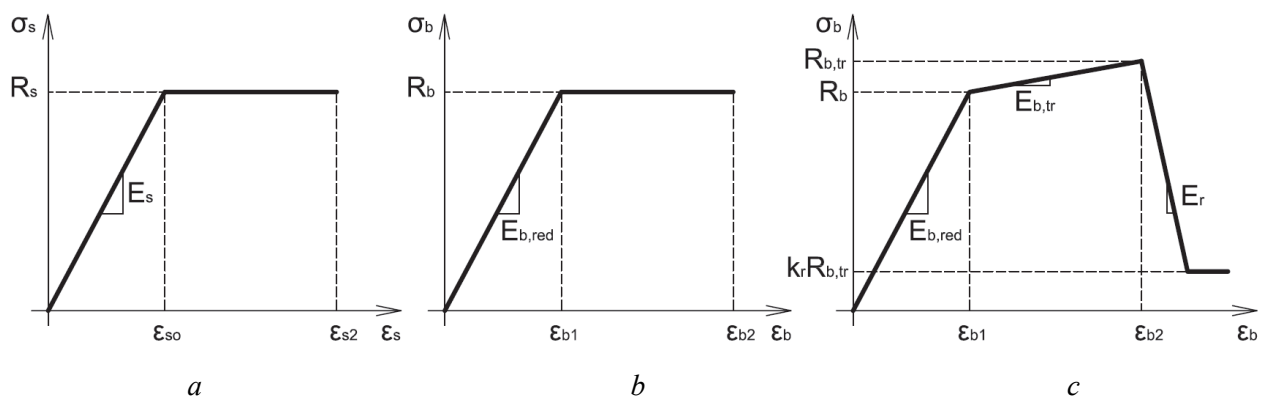
Figure 2. Deformation diagrams of materials:
a – reinforcement; *b* – unconfined concrete; *c* – confined concrete

Another approach would be to plot the diagrams based on taking into account the dissipation energy on the oscillation cycle. In this case, the dissipation energy can have either a constant value [16] or it can decrease with time based on the experimental dependence [17]. This approach allows a more accurate account of the energy dissipated by the structure at each cycle, however, it has the same drawbacks as the first one.

A more accurate way of setting the monotonic curve is the method based on the analysis of the stages of the stress-strain state (STS) of a reinforced concrete element. The procedure of the method is based on the identification of reference points in the diagram where the change in stiffness is observed. In this case, forces and displacements can be found both analytically and numerically. For bendable reinforced concrete elements such a diagram has been obtained in [18], which, however, does not take into account the branch of softening after reaching the limit force.

In this paper, the method based on the stages of the stress-strain diagram for the monotonic deformation of reinforced concrete columns is used to construct a monotonic deformation diagram. This approach is a generali-

zation of the method of ultimate forces, which is accepted in domestic and foreign design standards, taking into account the specific features of work of reinforced concrete element at the stage of failure: the value of axial load, the presence of indirect reinforcement in the form of clamps, concrete spalling of protective layer, loss of stability of compressed reinforcement, the presence of residual carrying capacity.

Methods and materials

As noted above, the basis for constructing a monotonic diagram will be to consider the actual deformation pattern of the reinforced concrete column and to identify the characteristic stages at which the stiffness will change and the transition to a new stage of the stress-strain state will be observed.

The monotonic diagram will be plotted in the axis "bending moment M – curvature ρ". For a given column, the longitudinal force N is assumed to be constant during all loading phases. Such a diagram can serve as a basis for the transition to the horizontal force-displacement relation, in which case not only the bending stiffness but also the shear stiffness must be considered, and the displacements caused by the slip of the reinforcement must also be taken into account [18].

The diagram is based on a number of general assumptions inherent to the limit force method:

– flat section hypothesis – the cross-sections are flat before deformation and remain so afterwards;

– the following state diagrams are adopted for the materials: bilinear for compressed concrete (Figure 2, *a*) and reinforcement (Figure 2, *b*); three-linear for concrete bounded by transverse collars (Figure 2, *c*) [19];

– geometric non-linearity caused by the longitudinal bending of the reinforced concrete column is taken into account by means of an appropriate coefficient η;

– the work of the tensile concrete is taken into account only at stage 1 – before the formation of cracks;

– stresses in concrete and reinforcement are found by composing and solving equations of equilibrium.

Assumptions made at specific stages will be described in the course of the presentation.

A general view of the deformation diagram of a reinforced concrete column is shown in (Figure 3). The diagram has 6 characteristic stages of deformation. Consider each stage separately and determine corresponding values of ultimate bending moment and curvature.
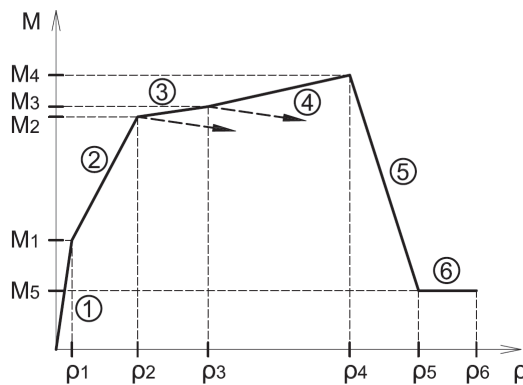

Figure 3. General view of reinforced concrete column deformation model

At the 1st stage (before cracking) the reinforcement and concrete in the tensile zone will be deformed together. The stress profile in the tensile concrete is non-linear trapezoidal and the highest stresses reach the design tensile strength of concrete R_{bt} (Figure 4, *a*). Compressed concrete works elastically, stress diagrams have a triangular shape. The ultimate bending moment at stage 1 is given by the equation

$$M_1 = R_{bt}W_{\text{pl}} + Ne_x, \qquad (1)$$

where W_{pl} – elastic-plastic moment of resistance of the section;

$$W_{\text{pl}} = 1,3W_{\text{red}}; \qquad (2)$$

e_x – distance from the core point furthest from the tensile face to the force application point *N*;

$$e_x = \frac{W_{\text{red}}}{A_{\text{red}}}. \tag{3}$$

The curvature corresponding to the moment M_1 is determined by the equation

$$\rho_1 = \frac{M_1}{D_1}, \tag{4}$$

where D – bending stiffness of reinforced concrete section at stage 1;

$$D_1 = E_{b,\text{red}} I_{\text{red}}. \tag{5}$$

In formulae (1)–(5) the geometric characteristics of the reduced section (area A_{red}, moment of inertia I_{red}, resistance torque W_{red}) are determined taking into account the entire cross-section of concrete and reinforcement.

Stage 2 is characterised by the operation after the formation of cracks in the tensile zone. The ultimate force in this stage can be achieved in two cases: the stresses in the reinforcement reach the yield stress R_s (stage 2.1) or the stresses in the concrete throughout the compressed zone have reached their design resistance R_b (stage 2.2). As we know which case the ratio of the relative height of the compressed zone ξ to its boundary value determines ξ_R: $\xi \le \xi_R$ – case of large eccentricities (stage 2.1); $\xi > \xi_R$ – the case of small eccentricities (stage 2.2). Note here, however, that in the first case, unlike in the second, the element does not enter the fracture stage.

Consider stage 2.1 in more detail (Figure 4, *c*). As noted, the stresses in the reinforcement at this stage reach the design resistance R_s. Stresses in the compressed concrete and in the compressed reinforcement do not exceed the corresponding design resistance R_b and R_{sc}. The compressive stresses in the concrete are assumed to be triangular.

The values of the stresses in the concrete and the compressed reinforcement are then determined from the consideration of the deformations in the flat section (flat section hypothesis). If at stage 2.1 the deformations in the tensile reinforcement reach a value of $\varepsilon_s = \varepsilon_{so}$, then the required stresses are found from the expressions

$$\sigma_b = E_{b,\text{red}} \frac{\varepsilon_{so} x}{h_o - x} \le R_b; \tag{6}$$

$$\sigma_{sc} = E_s \frac{\varepsilon_{so}(x - a')}{h_o - x} \le R_{sc}. \tag{7}$$

The symbols used in formulae (6) and (7) are given in Figure 4, *c*.

Note that if the stresses in formula (6) exceed the design resistance, then the stress diagram should be corrected by taking it in trapezoidal form, whereby the boundary between the triangular and rectangular parts of the diagram will be the fiber where the condition is fulfilled $\varepsilon_b = \varepsilon_{b1}$. Composing the equilibrium conditions for the internal forces and the moments of these forces with respect to the center of gravity of the stretched reinforcement, we find the height of the concrete compressed zone and the ultimate bending moment

$$x = \frac{N + R_s A_s - \sigma_{sc} A_s'}{0.5\sigma_b b}; \tag{8}$$

$$Ne_{2.1} = \sigma_{sc} A_s'(h_o - a') + \frac{1}{2}\sigma_b x b (h_o - \frac{x}{3}), \tag{9}$$

where A_s and A_s' – the areas of tensile and compressed reinforcement respectively.

The limiting bending moment with respect to the center of gravity will be found by taking into account the effects of longitudinal bending

$$M_i = \frac{Ne_i - N\dfrac{h_o - a'}{2}}{\eta},$$ (10)

where i – index denoting the stress train stage number; η – coefficient longitudinal bending

$$\eta_i = \frac{1}{1 - \dfrac{N}{N_{cr_i}}},$$ (11)

where N_{cr_i} – critical force at i stage;

$$N_{cr_i} = \frac{\pi^2 D_i}{l_o^2},$$ (12)
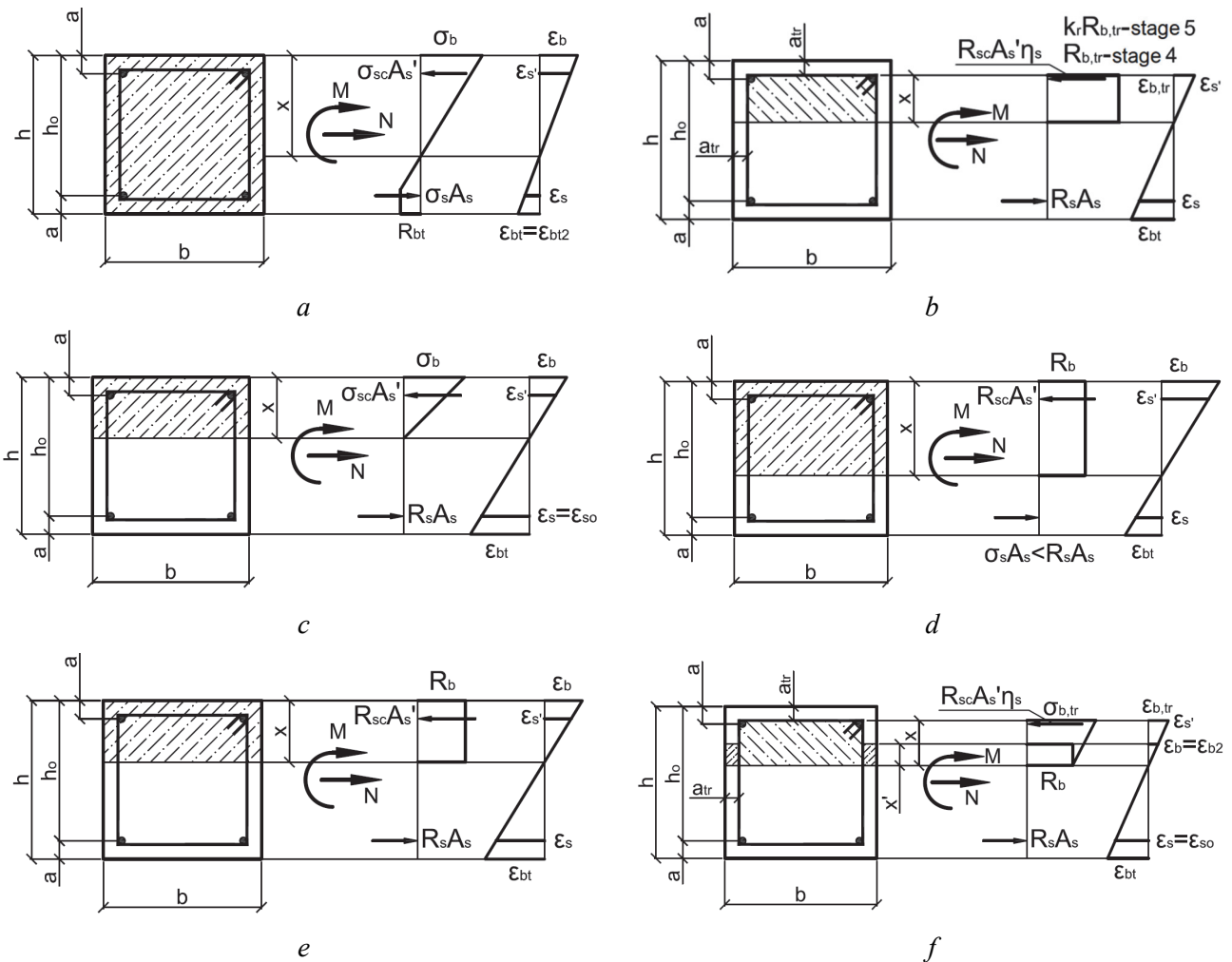
where l_o – design element length.

Figure 4. Stages of the stress-strain state of a reinforced concrete column:
a – stage 1; *b* – stages 4 and 5; *c* – stage 2.1; *d* – stage 2.2; *e* – stage 3.1; *f* – stage 3.2

Stiffness in this and subsequent stages D_i we find with the variable height of the compression zone x_m and tensile concrete work between cracks, which is taken into account by the coefficient ψ_s. The relevant formulas are described in sufficient detail in the regulatory literature (SP63.13330.2018. Concrete and reinforced concrete structures) and, due to their cumbersome nature, are not given in the text of this article.

Stage 2.2 will in turn correspond to the failure stage of the reinforced concrete section for the case of small eccentricities. The stresses in the compressed concrete are distributed according to a rectangular law and are equal to the design resistance R_b, in the compressed reinforcement, the stresses also reach the design resistance R_{sc}, and in the stretched one less than the value R_s (Figure 4, *d*). Composing and transforming the equilibrium equations we find

$$x = \frac{N + R_s A_s \dfrac{1+\xi_R}{1-\xi_R} - R_{sc} A_s'}{R_b b + \dfrac{2 R_s A_s}{h_o (1-\xi_R)}};$$ (13)

$$Ne_{2.2} = R_{sc} A_s'(h_o - a') + R_b x b(h_o - 0,5x).$$ (14)

The limiting bending moment and curvature will be obtained from formulae (4) and (10).

Stage 3 will also be considered in two variants. In stage 3.1, for elements operating with large eccentricities, a subsequent increase in bending moment due to the yield strength of the tensile reinforcement will result in an increase in compressive stresses in the concrete to the value of R_b and stresses in the compressed reinforcement up to R_{sc} (Figure 4, *e*). The reinforced concrete section will enter the fracture stage. From the equilibrium conditions we have

$$x = \frac{N + R_s A_s - R_{sc} A_s'}{R_b b};$$ (15)

$$Ne_{3.1} = Ne_{2.2}.$$ (16)

In turn, if the element failed at low eccentricities, a transition to stage 3.2 will follow (Figure 4, *f*). The deformation in this stage will take place until the yield point is reached in the stretched reinforcement. The compressed zone of the concrete will be divided into two parts: a protective layer and a concrete core bounded by transverse collars. If the bending moment increases, the concrete protective layer for the fibers will splinter off, where the relative deformations of the unconfined concrete reach the limit values $\varepsilon_b = \varepsilon_{b2}$. Then only the height of the compressed concrete protection layer will be taken into account in the calculation x'.

At this stage the indirect reinforcement is activated, as a result of which the stresses in the concrete core will increase. The compressive stress profile is assumed to be trapezoidal with a minimum value at the neutral fibre equal to R_b and maximum value $\sigma_{b,tr}$.

Applying the plane section hypothesis, determine the values of x' and $\sigma_{b,tr}$ considering that the relative deformations in the reinforcement reach the limit values $\varepsilon_s = \varepsilon_{so}$

$$x' = \frac{\varepsilon_{b2}(h_o - x - a_{tr})}{\varepsilon_{so}};$$ (17)

$$\sigma_{b,tr} = E_{b,tr} \frac{\varepsilon_{so} x}{h_o - x - a_{tr}}.$$ (18)

Composing and solving the equilibrium equations we obtain

$$x = \frac{N + R_s A_s - R_{sc} A_s' \eta_s - 2R_b x' a_{tr}}{0,5b(R_b + \sigma_{b3})}; \tag{19}$$

$$Ne_{3.2} = R_{sc} A_s' \eta_s (h_o - a') + 2R_b x' a_{tr} (h_o - x - a_{tr} + 0,5x') + R_b xb(h_o - a_{tr} - 0,5x) +$$
$$+ \frac{1}{2}(\sigma_{b,tr} - R_b)xb(h_o - a_{tr} - \frac{x}{3}), \tag{20}$$

where $\eta_s = 0–1$ – a coefficient which takes into account the reduced contribution to the load-bearing capacity of the part of reinforcement bars which have lost stability due to ineffective retention by transverse reinforcement in the free-bending section of the clamp.

It is important to note that in stage 3.2 it is possible to increase the bending moment limit as well as to decrease it. This depends on the fraction of the resistance that the cross-section loses when the concrete protection layer rebounds and part of the compressed reinforcement becomes unstable. In Figure 3 the possible directions of unstrengthening are shown by the dotted arrow lines.

At stage 4, the load-bearing capacity of the section will be exhausted. As the bending moment increases, the stresses in the concrete core will reach their design resistance $R_{b,tr}$, which will be accompanied by the transverse clamps flowing (Figure 4, *b*).

The strength of confined concrete $R_{b,tr}$ depends on the strength of unconfined concrete R_b and the effective lateral pressure R_e which results from the resistance of the clamps to the transverse deformations of concrete. According to [12] the strength of confined concrete can be determined as

$$R_{b,tr} = R_b + 4,1R_e. \tag{21}$$

The effective lateral pressure R_e in the case of a square cross-section is

$$R_e = k_e \rho_s R_{sw}, \tag{22}$$

where R_{sw} – yield strength of transverse reinforcement; k_e – retention factor, which takes into account the uneven compression of concrete in cross-sections other than circular; ρ_s – transverse reinforcement coefficient by volume.

In view of the considerable deformations in the cross-section and the consequent low height of the compressed zone x', the component related to the resistance of the unconfined concrete at this stage will be neglected.

Composing and solving the equilibrium equations we obtain

$$x = \frac{N + R_s A_s - R_{sc} A_s' \eta_s}{R_{b,tr} b}; \tag{23}$$

$$Ne_4 = R_{sc} A_s' \eta_s (h_o - a') + R_{b,tr} xb(h_o - a_{tr} - 0,5x). \tag{24}$$

At stage 5, the load-bearing capacity of the reinforced concrete cross-section will be reduced, which is reflected in the diagram by the presence of a softening branch. Stresses in the concrete core will decrease to the value of $k_r R_{b,tr}$, where k_r – is the residual strength factor of the confined concrete (Figure 4, *b*). Otherwise, the design dependencies will be similar to the corresponding ones in stage 4.

The curvature in stage 6 will increase with a constant value of bending moment until the longitudinal or transverse reinforcement reaches the limit of relative strain ε_{s2}, which will be accompanied by a rupture of the reinforcement and complete exhaustion of the load-bearing capacity.

It is worth noting that the latter criterion must be monitored at all stress-strain stages.

Results and discussion

The dependencies obtained will be considered on the example of a reinforced concrete column of a frame structure. We will carry out the calculation in two variants – with the coefficient of longitudinal force $\nu = 0,3$ and $\nu = 0,6$.

$$\nu = \frac{N}{R_b A_b}.$$ (25)
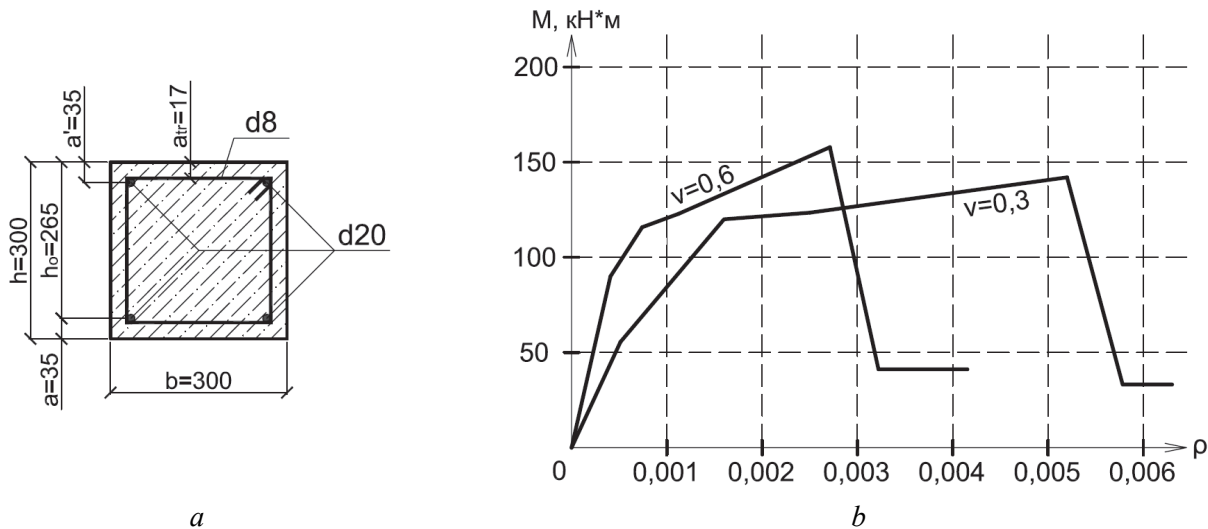
Figure 5. Cross-section of a reinforced concrete column (*a*)
and "moment – curvature" diagrams based on the results of calculations based on the proposed model (*b*)

The cross-section of the column is square 300×300 mm, the geometric dimensions are given in Figure 5, *a*. Longitudinal reinforcement of 4 bars $\varnothing$25A400, $A_s = A_s' = 982$ mm². Cross reinforcement from $\varnothing$8A400 with pitch $s_w = 100$ mm, $\rho_s = 0,005$.

The design length of the column is assumed to be $l_o = 3$ m. Consider all reinforcement effectively secured against loss of stability $\eta_s = 1$. The residual strength coefficient is assumed to be $k_r = 0,25$ [20]. Concrete class B20.

The calculation results are shown in Figure 5, *b*. It can be seen from the graphs that the ultimate bearing capacity for the column with a higher longitudinal force coefficient ν higher, although this column shows less load-bearing capacity prior to the failure of the protective layer than with $\nu = 0,3$.

It should be noted that due to the inclusion of the compressed zone of concrete in the work, the more loaded column has greater stiffness in all stress-strain stages. While the less loaded column shows greater capacity for plastic deformation, especially at the stage after the inclusion of indirect reinforcement.

Residual load-bearing capacity for column at $\nu = 0,6$ is slightly higher. Failure in both cases is due to clamp rupture when the relative strain limits are reached.

Conclusion

The analytical model for construction of monotone diagram "moment – curvature" for reinforced concrete columns at different level of axial load, taking into account indirect reinforcement by transverse collars, loss of stability of compressed reinforcement, residual strength of concrete is obtained. The model takes into account all stages of the static deformation of eccentrically compressed reinforced concrete elements, including the non-critical phases of operation. The model can also be used for calculation of frame beams.

The authors consider that the main purpose of constructing such a monotonic diagram is to use it as a basis for a hysteresis diagram which describes the behaviour of reinforced concrete elements under low cycle seismic loads. It is worth considering that bringing reinforced concrete elements to supercritical stages, when there is destruction of concrete protective layer and loss of stability of compressed rods, is not always justified in terms of efficiency of repair and further operation of structure. But when designing buildings based on the concept of non-destruction, the proposed model will allow to reveal reserves of bearing capacity of the system.

The developed model is suitable for solving by hand calculation, however in case of more complex deformation, e.g. oblique eccentric compression, section damage due to fire or corrosion, sections other than rectangular shape it is possible to apply for solving equilibrium equations at each stage a non-linear deformation model.

References

1. Tamrazyan A.G., Chernik V.I. Consideration of the effects of fire in the design of reinforced concrete buildings in earthquake-prone areas. *Proceedings XIV Russian National Conference on Earthquake Engineering and Seismic Zoning (with International Participation)*. Sochi, Moscow; 2021. p. 114–117. (In Russ.) https://doi.org/10.37153/2687-0045-2021-14-114-117

2. Tamrazyan A.G., Avetisyan L.A. Behavior of compressed reinforced concrete columns under thermodynamic influences taking into account increased concrete deformability. *IOP Conference Series: Materials Science and Engineering.* 2018;365:052034. https://doi.org/10.1088/1757-899X/365/5/052034

3. Tamrazyan A., Popov D. Reduce of bearing strength of the bent reinforce-concrete elements on a sloping section with the corrosive damage of transversal armature. *MATEC Web of Conferences.* 2017;117:00162. https://doi.org/10.1051/matecconf/201711700162

4. Sengupta P., Li B. Hysteresis modeling of reinforced concrete structures: state of the art. *ACI Structural Journal.* 2017;114(1):25–38. https://doi.org/10.14359/51689422

5. Veletsos A.S., Newmark N.M., Chelapati C.V. Deformation spectra for elastic and elastoplastic systems subjected to ground shock and earthquake motions. *Proceedings of 3rd World Conference on Earthquake Engineering.* 1965;V(II):663–682.

6. Chernik V.I. Effective stiffness of reinforced concrete columns after a fire. *Science Prospects.* 2022;(5):82–86. (In Russ.)

7. Takeda T., Sozen M.A., Nielson N.N. Reinforced concrete response to simulated earthquakes. *Journal of the Structural Division, ASCE.* 1970;96:2557–2573.

8. Clough R.W., Johnston S.B. Effect of stiffness degradation on earthquake ductility requirements. *Proceedings of 2nd Japan National Conference on Earthquake Engineering.* Tokyo; 1966. p. 227–232.

9. Imbeault F.A., Nielsen N.N. Effect of degrading stiffness on the response of multistory frames subjected to earthquakes. *Proceedings of 5th World Conference on Earthquake Engineering, Rome, 26–29 June 1973.* Rome; 1973. p. 1756–1765.

10. Saidi M., Sozen M.A. *Simple and complex models for nonlinear seismic response of reinforced concrete structures. A report to the National Science Foundation, University of Illinois at Urbana-Champaign.* Champaign; 1979.

11. Ozcebe G., Saatcioglu M. Hysteresis shear models for reinforced concrete members. *Journal of Engineering Mechanics.* 1989;115(1):132–148.

12. Mander J.B., Priestley J.N., Park R. Theoretical stress-strain model for confined concrete. *Engineering Structures.* 1989;116:1804–1825.

13. Dowell R.K., Seible F., Wilson E.L. Pivot hysteresis model for reinforced concrete members. *ACI Structural Journal, ASCE.* 1998;95(5):607–617.

14. Tamrazyan A., Chernik V. Equivalent viscous damping ratio for a RC column under seismic load after a fire. *IOP Conference Series: Materials Science and Engineering.* 2021;1030:012095. https://doi.org/10.1088/1757-899X/1030/1/012095

15. Ibarra L.F., Medina R.A., Krawinkler H. Hysteretic models that incorporate strength and stiffness deterioration. *Earthquake Engineering& Structural Dynamics.* 2005;34(12):1489–1511. https://doi.org/10.1002/eqe.495

16. Bondarenko V.M., Yagupov B.A. About connection between force load level and energy losses at deformation of reinforced concrete structures. *Structural Mechanics of Engineering Constructions and Buildings.* 2016;(3):44–50. (In Russ.)

17. Sucuoglu H., Erberik A. Energy-based hysteresis and damage models for deteriorating systems. *Earthquake Engineering & Structural Dynamics.* 2004;33(1):69–88. https://doi.org/10.1002/eqe.338

18. Moehle J. *Seismic design of reinforced concrete buildings.* McGraw-Hill; 2014.

19. Tamrazyan A.G., Manaenkov I.K. To calculation of bendable reinforced concrete elements with indirect reinforcement of compressed zone. *Industrial and Civil Engineering.* 2016;(7):41–44. (In Russ.)

20. Chernik V.I., Samarina S.E. Numerical model of a compressed concrete element strengthened by FRP jackets. *Building and Reconstruction.* 2020;(1):40–53. (In Russ.) https://doi.org/10.33979/2073-7416-2020-87-1-40-53